



FEASIBILITY STUDY OF APPLYING LAMINAR FLOW CONTROL  
TO AN LTA VEHICLE

Dwight J. Warner, Suphi A. Ozgur, and Wayne W. Haigh  
DYNAMICS TECHNOLOGY, INC.  
22939 Hawthorne Boulevard, Suite 200  
Torrance, California 90505

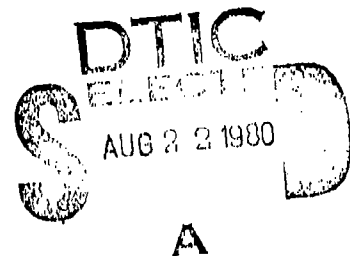
April 1980

FINAL REPORT  
CONTRACT NO. N00140-79-C-6565 (P00003)

Approved for Public Release; Distribution Unlimited

Prepared for  
NAVAL AIR DEVELOPMENT CENTER  
Aircraft and Crew Systems Technology Directorate  
WARMINSTER, PENNSYLVANIA 18974

Through an Interagency Agreement with  
NAVAL UNDERWATER SYSTEMS CENTER  
NEWPORT, RHODE ISLAND 02840



80 8 21 044

AD A088148

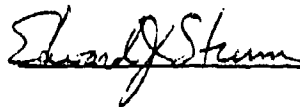
BUUC FILE COPY

## NOTICES

REPORT NUMBERING SYSTEM - The numbering of technical project reports issued by the Naval Air Development Center is arranged for specific identification purposes. Each number consists of the Center acronym, the calendar year in which the number was assigned, the sequence number of the report within the specific calendar year, and the official 2-digit correspondence code of the Command Office or the Functional Directorate responsible for the report. For example: Report No. NADC-78015-20 indicates the fifteenth Center report for the year 1978, and prepared by the Systems Directorate. The numerical codes are as follows:

CODE	OFFICE OR DIRECTORATE
00	Commander, Naval Air Development Center
01	Technical Director, Naval Air Development Center
02	Comptroller
10	Directorate Command Projects
20	Systems Directorate
30	Sensors & Avionics Technology Directorate
40	Communication & Navigation Technology Directorate
50	Software Computer Directorate
60	Aircraft & Crew Systems Technology Directorate
70	Planning Assessment Resources
80	Engineering Support Group

APPROVED BY:



DATE:



UNCLASSIFIED

SECURITY CLASSIFICATION OF THIS PAGE (When Data Entered)

19. REPORT DOCUMENTATION PAGE		READ INSTRUCTIONS BEFORE COMPLETING FORM
1. REPORT NUMBER (18) NADC-80144-60	2. GOVT ACCESSION NO. AD-A088	3. RECIPIENT'S CATALOG NUMBER 248
4. TITLE (and Subtitle) (16) Feasibility Study of Applying Laminar Flow Control to an LTA Vehicle.		5. TYPE OF REPORT & PERIOD COVERED (17) Final Report
7. AUTHOR(s) (10) Dwight J. Warner, Suphi A. Ozgur, and Wayne W. Haigh		6. PERFORMING ORG. REPORT NUMBER (14) DT-7909-14
9. PERFORMING ORGANIZATION NAME AND ADDRESS Dynamics Technology, Inc. 22939 Hawthorne Boulevard, Suite 200 Torrance, CA 90505		8. CONTRACT OR GRANT NUMBER(s) (13) N00140-79-C-6565/P00003
11. CONTROLLING OFFICE NAME AND ADDRESS Naval Air Development Center; Aircraft and Crew Systems Technology Directorate (Code 605B); Warminster, PA 18974		10. PROGRAM ELEMENT, PROJECT, TASK AREA & WORK UNIT NUMBERS P.E. 62241N; AIRTASK A03P-03PA-001B/OF41-411-000; W.U. DH-832
14. MONITORING AGENCY NAME & ADDRESS (if different from Controlling Office) Naval Underwater Systems Center Newport, RI 02840 (17) WP42411008		12. REPORT DATE (11) Apr 1980
		13. NUMBER OF PAGES 45
		15. SECURITY CLASS. (of this Report) UNCLASSIFIED
		15a. DECLASSIFICATION/DOWNGRADING SCHEDULE
16. DISTRIBUTION STATEMENT (of this Report)  Approved for Public Release; Distribution Unlimited		
17. DISTRIBUTION STATEMENT (of the abstract entered in Block 20, if different from Report)		
18. SUPPLEMENTARY NOTES		
19. KEY WORDS (Continue on reverse side if necessary and identify by block number)  Aerodynamic Drag Boundary Layer Control Lighter-Than-Air Vehicle		
20. ABSTRACT (Continue on reverse side if necessary and identify by block number)  The feasibility of applying laminar boundary-layer control with body shaping to a high altitude, Lighter-Than-Air vehicle was investigated. Solar radiation-induced surface heating was shown to have a destabilizing effect on laminar flow and caused the laminar flow to break down on regions of the vehicle surface exposed to high levels of solar radiation. Aerodynamic drag estimates were made for the vehicle. Surface waviness and roughness criteria for achieving laminar flow were determined.		

SECURITY CLASSIFICATION OF THIS PAGE(When Data Entered)

SECURITY CLASSIFICATION OF THIS PAGE(When Data Entered)

FOREWORD

This report is the Final Technical Report for Contract N00140-79-C-6565, Amendment P00003 . This feasibility study was sponsored by the Naval Air Development Center (NADC), Warminster, Pennsylvania, and was administered by the Naval Underwater Systems Center, Newport, Rhode Island (Mr. Richard H. Nadolink, IPUV Program Manager); through an interagency agreement with NADC. This contractual effort was performed between January 1980 and April 1980. The NADC Program Monitors were Mr. Samuel Greenhalgh and Mr. John A. Eney of the Lighter-Than-Air Systems Technology Office; the Program Manager for Dynamics Technology was Wayne W. Haigh. This Final Report completes the data requirements of the contract.

Accession For	
1.1	<input checked="checked" type="checkbox"/>
1.2	<input type="checkbox"/>
1.3	<input type="checkbox"/>
1.4	<input type="checkbox"/>
1.5	<input type="checkbox"/>
1.6	<input type="checkbox"/>
1.7	<input type="checkbox"/>
1.8	<input type="checkbox"/>
1.9	<input type="checkbox"/>
1.10	<input type="checkbox"/>
1.11	<input type="checkbox"/>
1.12	<input type="checkbox"/>
1.13	<input type="checkbox"/>
1.14	<input type="checkbox"/>
1.15	<input type="checkbox"/>
1.16	<input type="checkbox"/>
1.17	<input type="checkbox"/>
1.18	<input type="checkbox"/>
1.19	<input type="checkbox"/>
1.20	<input type="checkbox"/>
1.21	<input type="checkbox"/>
1.22	<input type="checkbox"/>
1.23	<input type="checkbox"/>
1.24	<input type="checkbox"/>
1.25	<input type="checkbox"/>
1.26	<input type="checkbox"/>
1.27	<input type="checkbox"/>
1.28	<input type="checkbox"/>
1.29	<input type="checkbox"/>
1.30	<input type="checkbox"/>
1.31	<input type="checkbox"/>
1.32	<input type="checkbox"/>
1.33	<input type="checkbox"/>
1.34	<input type="checkbox"/>
1.35	<input type="checkbox"/>
1.36	<input type="checkbox"/>
1.37	<input type="checkbox"/>
1.38	<input type="checkbox"/>
1.39	<input type="checkbox"/>
1.40	<input type="checkbox"/>
1.41	<input type="checkbox"/>
1.42	<input type="checkbox"/>
1.43	<input type="checkbox"/>
1.44	<input type="checkbox"/>
1.45	<input type="checkbox"/>
1.46	<input type="checkbox"/>
1.47	<input type="checkbox"/>
1.48	<input type="checkbox"/>
1.49	<input type="checkbox"/>
1.50	<input type="checkbox"/>
1.51	<input type="checkbox"/>
1.52	<input type="checkbox"/>
1.53	<input type="checkbox"/>
1.54	<input type="checkbox"/>
1.55	<input type="checkbox"/>
1.56	<input type="checkbox"/>
1.57	<input type="checkbox"/>
1.58	<input type="checkbox"/>
1.59	<input type="checkbox"/>
1.60	<input type="checkbox"/>
1.61	<input type="checkbox"/>
1.62	<input type="checkbox"/>
1.63	<input type="checkbox"/>
1.64	<input type="checkbox"/>
1.65	<input type="checkbox"/>
1.66	<input type="checkbox"/>
1.67	<input type="checkbox"/>
1.68	<input type="checkbox"/>
1.69	<input type="checkbox"/>
1.70	<input type="checkbox"/>
1.71	<input type="checkbox"/>
1.72	<input type="checkbox"/>
1.73	<input type="checkbox"/>
1.74	<input type="checkbox"/>
1.75	<input type="checkbox"/>
1.76	<input type="checkbox"/>
1.77	<input type="checkbox"/>
1.78	<input type="checkbox"/>
1.79	<input type="checkbox"/>
1.80	<input type="checkbox"/>
1.81	<input type="checkbox"/>
1.82	<input type="checkbox"/>
1.83	<input type="checkbox"/>
1.84	<input type="checkbox"/>
1.85	<input type="checkbox"/>
1.86	<input type="checkbox"/>
1.87	<input type="checkbox"/>
1.88	<input type="checkbox"/>
1.89	<input type="checkbox"/>
1.90	<input type="checkbox"/>
1.91	<input type="checkbox"/>
1.92	<input type="checkbox"/>
1.93	<input type="checkbox"/>
1.94	<input type="checkbox"/>
1.95	<input type="checkbox"/>
1.96	<input type="checkbox"/>
1.97	<input type="checkbox"/>
1.98	<input type="checkbox"/>
1.99	<input type="checkbox"/>
1.100	<input type="checkbox"/>

A

TABLE OF CONTENTS

	<u>PAGE</u>
FOREWORD.....	ii
TABLE OF CONTENTS.....	iii
LIST OF FIGURES.....	iv
LIST OF TABLES.....	v
1. INTRODUCTION.....	1
2. DESIGN CONDITIONS FOR AN OPERATIONAL LTA VEHICLE.....	3
3. LAMINAR FLOW LTA VEHICLE DESIGN.....	7
4. BOUNDARY-LAYER ANALYSIS INCLUDING SOLAR RADIATION.....	12
5. LTA VEHICLE DRAG ESTIMATES.....	19
5.1 Hull Drag Estimates.....	19
5.2 Fin Drag Estimates.....	22
5.3 Gondola Drag Estimates.....	24
5.4 Interference and Support Wire Drag Estimates.....	27
5.5 Total Drag Estimates for the LTA Vehicle.....	28
6. VEHICLE DESIGN CONSIDERATIONS.....	30
7. SUMMARY AND RECOMMENDATIONS.....	34
8. REFERENCES.....	36
APPENDIX A. MIXED FLOW DRAG ANALYSIS METHOD.....	A1

LIST OF FIGURES

<u>FIGURE</u>	<u>PAGE</u>
1. Wind Speed/Frequency Distributions for Two Locations and Altitudes.....	4
2. Unit Reynolds Number as a Function of Vehicle Speed and Altitude.....	5
3. Geometry and Pressure Distribution of the Selected LTA Vehicle.....	8
4. Boundary-Layer Stability Results for the Selected LTA Vehicle at Adiabatic Conditions.....	10
5. Equilibrium Surface Temperature Distribution for the LTA Vehicle.....	15
6. Boundary-Layer Shape Factor Variation for the LTA Vehicle Including Effects of Solar Radiation.....	16
7. End View Schematic of Vehicle Showing Turbulent and Laminar Flow Regions.....	18
8. Schematic of the Vehicle Showing Geometry of Turbulent Flow...	21
9. Control Fin Configurations for the LTA Vehicle.....	23
10. Schematic of the Gondola-Hull Junction.....	25
11. Allowable Roughness Height for the LTA Vehicle.....	31

LIST OF TABLES

<u>TABLE</u>	<u>PAGE</u>
1. Hull Drag Estimates for Specified Flow Conditions.....	22
2. Fin Drag Estimates for Two Fin Configurations.....	24
3. Gondola Drag Estimates.....	27
4. LTA Vehicle Total Drag Estimates.....	28



## 1. INTRODUCTION

The United States Navy sponsored a program to develop a high altitude Lighter-Than-Air (LTA) vehicle in recent years with a vehicle denoted as HASPA (High Altitude Superpressured Powered Aerostat). HASPA was designed, fabricated, and tested in two flight tests in the period from 1974 through early 1976 (Scales and McComas, 1977). These flight tests were plagued with problems related to structural failure of the hull material. Field operations were terminated in August 1976 as a result of these problems and a material improvement program was initiated. In addition, a review of the wind speed/frequency distributions at the proposed operational altitudes indicated that the design speed capability of HASPA was not sufficient to maintain station throughout the year, and therefore, low drag hull studies were initiated.

One such study, which is documented in Marcy and Hookway (1979), investigated the use of laminar flow control for the High Altitude Surveillance Platform for Over-The-Horizon Targeting (HI-SPOT) vehicle. This study identified the endurance and relative wind speed advantages inherent in a pressure gradient stabilized laminar flow hull, however, it did not address the practical difficulties of utilizing this laminar flow control technique for this mission.

The primary objective of the present study was to investigate the feasibility of applying laminar boundary-layer control with body shaping (pressure gradient) to an LTA Vehicle. In particular, this investigation includes an assessment of the effects of solar radiation on the ability to maintain laminar boundary-layer flow on a vehicle hull, and identifies the surface finish requirements and other constraints which must be met in the design of a laminar flow vehicle.

The operational conditions which impact on the design considerations of the LTA Vehicle are presented and discussed in Section 2. A laminar flow vehicle design is selected in Section 3 based on an advanced submersible configuration which has been successfully tested in a similar Reynolds number regime. Boundary-layer stability calculations are presented in this section which demonstrate that this vehicle configuration is an adequate design when the vehicle surface temperature is maintained at an adiabatic condition, such as during nighttime operation. A thermodynamic analysis of the effect of daytime solar radiation on the surface temperature of the hull and the associated effect of the heated surface on the laminar boundary-layer stability are discussed in Section 4. Drag estimates of the various LTA Vehicle components along with estimates of operational shaft horsepower levels, including comparisons with the HI-SPOT Vehicle, are presented in Section 5. Vehicle design considerations pertinent to laminar flow control are presented in Section 6, and a summary of the feasibility of utilizing laminar flow control on a high altitude LTA Vehicle, together with future recommendations are presented in Section 7.

## 2. DESIGN CONDITIONS FOR AN OPERATIONAL LTA VEHICLE

The LTA Vehicle of interest in the present study is intended to operate at altitudes between 55,000 feet and 70,000 feet and maintain station within a 50 nautical mile radius in winds up to speeds of 100 knots. Presented in Figure 1 are the wind speed/frequency distributions, obtained from Marcy and Hookway (1979), for two proposed operating locations; Keflavik, Iceland and Iraklion, Crete. These wind speed/frequency distributions are for the winter season of the year during which the wind speed magnitudes are largest. The altitudes of 55,000 feet and 70,000 feet represent the altitudes of minimum wind speed for these winter distributions at the two proposed operating locations. The wind speed at an altitude of 55,000 feet (nominal pressure of 100 mb) is below 79 knots 95 percent of the time, and the wind speed for an altitude of 70,000 feet (nominal pressure of 50 mb) is below 46 knots 95 percent of the time. Based on the above and additional information (Greenhalgh, 1980), a point design condition to maintain station corresponding to a relative wind speed of 80 knots and an altitude of 55,000 feet was chosen. The 80 knot wind speed is exceeded less than 4 percent of the time throughout the year, and therefore a vehicle designed to relative speeds of 80 knots should be able to maintain station under all but the most extreme wind conditions at these two proposed operating locations.

A family of curves showing unit Reynolds number,  $U_\infty/\nu$  as a function of vehicle relative speed,  $U_\infty$ , and operational altitude,  $H$ , is presented in Figure 2. This figure shows the strong influence of altitude variations on the unit Reynolds number. The laminar flow for a fixed vehicle shape is more stable at the lower unit Reynolds numbers, which result at the higher altitudes. By operating at the higher altitudes, 70,000 feet versus 55,000 feet, two beneficial effects occur which may reduce propulsion power requirements.\*

---

\* The only possible exception to this is if the wind speeds increase appreciably at the higher altitudes.

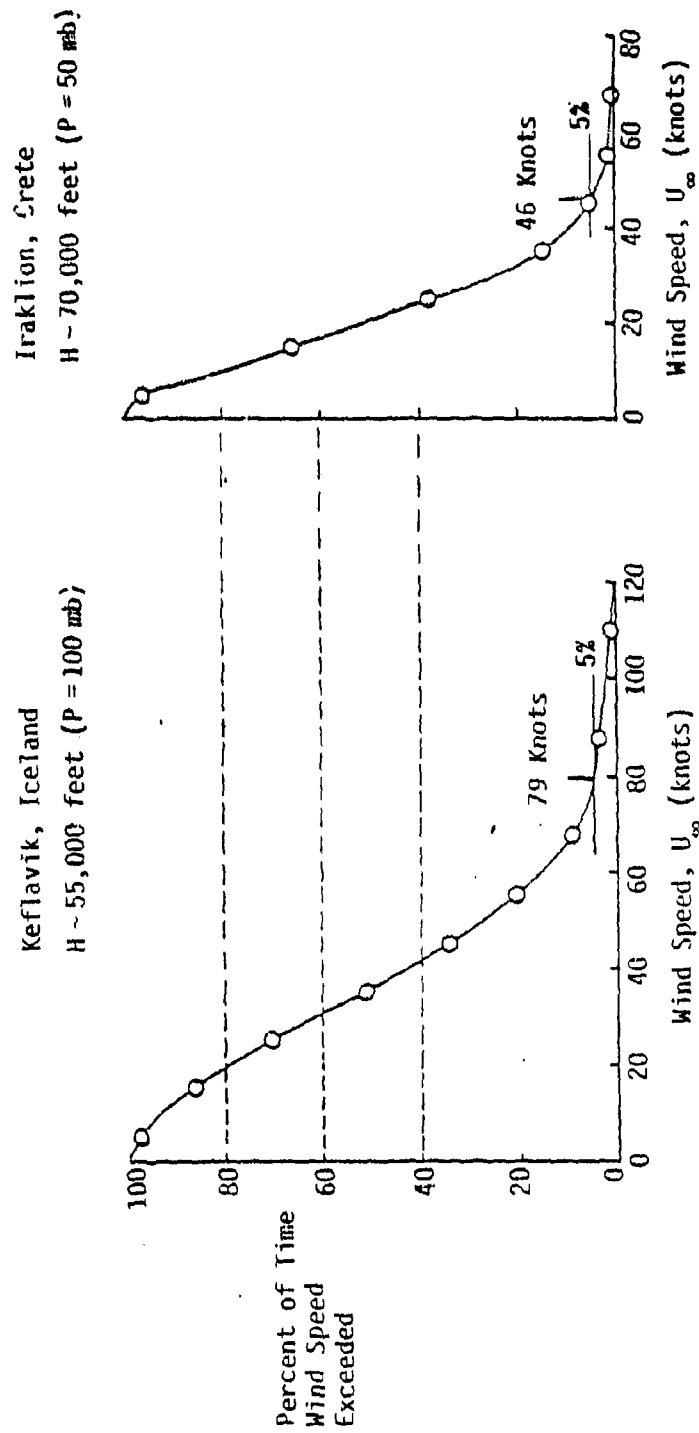


Figure 1. Wind Speed/Frequency Distributions for Two Locations and Altitudes.

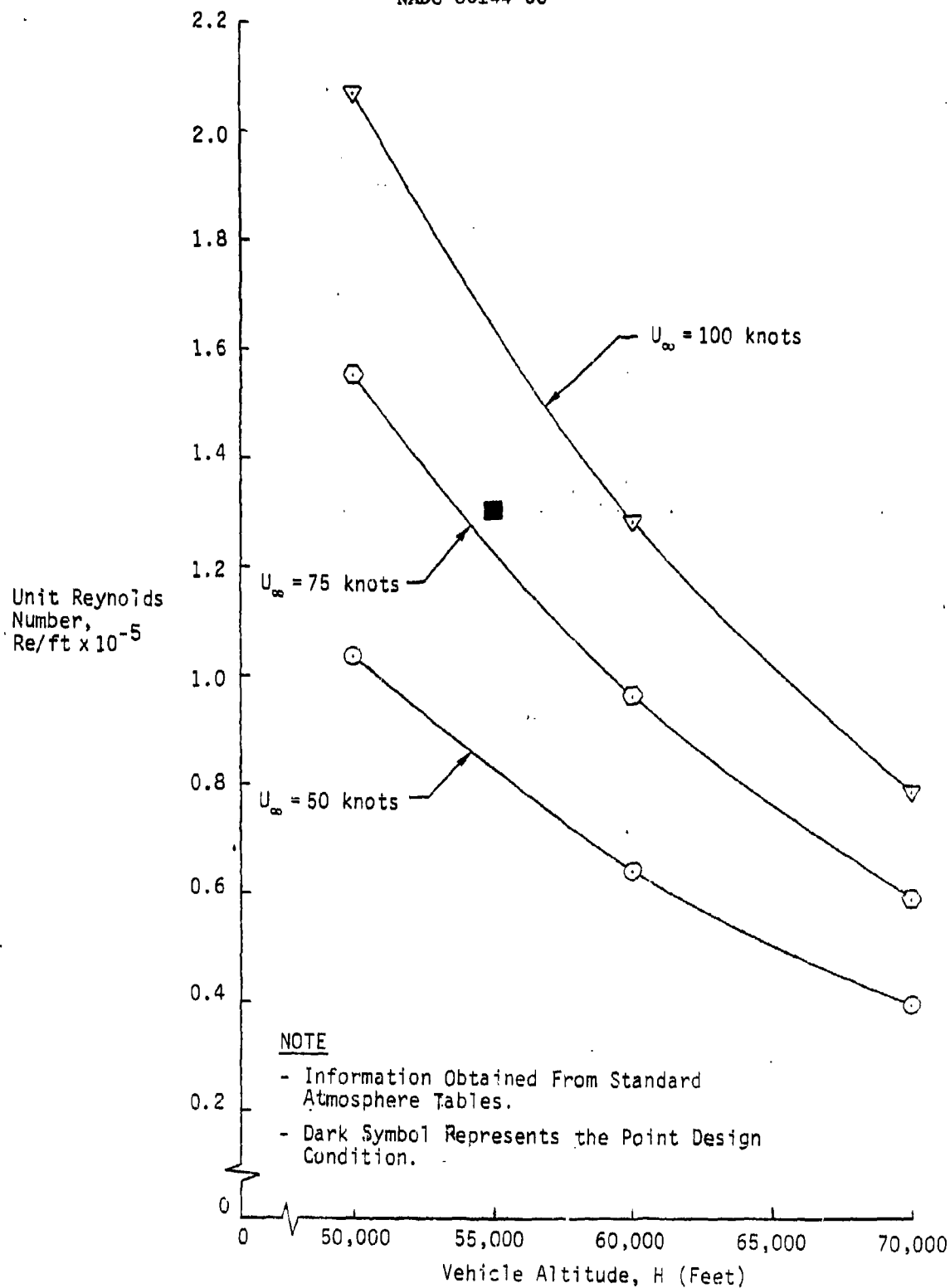


Figure 2. Unit Reynolds Number as a Function of Vehicle Speed and Altitude.

- The air density decreases by about a factor of 2 between 55,000 feet and 70,000 feet altitudes, and therefore the dynamic pressure will be reduced (for fixed velocity) and result in lower vehicle drag.
- The unit Reynolds number is lower at the higher altitude (for fixed velocity) and, therefore, a vehicle meeting laminar flow requirements is easier to design.

The solid symbol shown in Figure 2 shows the unit Reynolds number for the point design condition (speed of 80 knots and altitude of 55,000 feet.)

### 3. LAMINAR FLOW LTA VEHICLE DESIGN

The application of passive (body shaping) state-of-the-art laminar flow technology to an LTA Vehicle has been performed for an adiabatic\* vehicle at a freestream speed of 80 knots and an altitude of 55,000 feet.

The geometry and corresponding pressure distribution for the vehicle that has been applied to this mission is presented in Figure 3. This vehicle has a length of about 350 feet, a maximum diameter of about 85 feet, and a volume of 800,000 cubic feet. A favorable pressure gradient extends to an axial length of about 175 feet. This favorable pressure gradient provides the stabilizing mechanism by which laminar flow is maintained. The distance to which laminar flow is maintained is basically a function of the arc-length Reynolds number for a fixed favorable pressure gradient distribution. The configuration of the vehicle shown in Figure 3 is based on Vehicle B-1 which was designed as a submersible research vehicle (Hunt, 1977 and Haigh, Warner and Ozgur, 1980). This vehicle shape was chosen for application to the LTA Vehicle mission, since the maximum theoretical Reynolds number, for which laminar flow can be obtained with Vehicle B-1, is fairly similar to the operational Reynolds number requirement of the LTA Vehicle.

Baseline boundary-layer stability\*\* calculations were performed for this vehicle at adiabatic conditions using the TAPS Code (Gentry and Wazzan, 1976). The boundary-layer stability analysis contained in the TAPS Code is based upon a small disturbance linear theory, and it has been shown by Smith and Gamberoni (1956) and Jaffe, Okamura and Smith (1970) that

---

\* The effect of surface heating resulting from solar radiation, on laminar flow stability is discussed in Section 4 of this report.

\*\* The term stability (or stabilized) refers to the stability of the laminar flow, not vehicle control stability, unless otherwise specified.

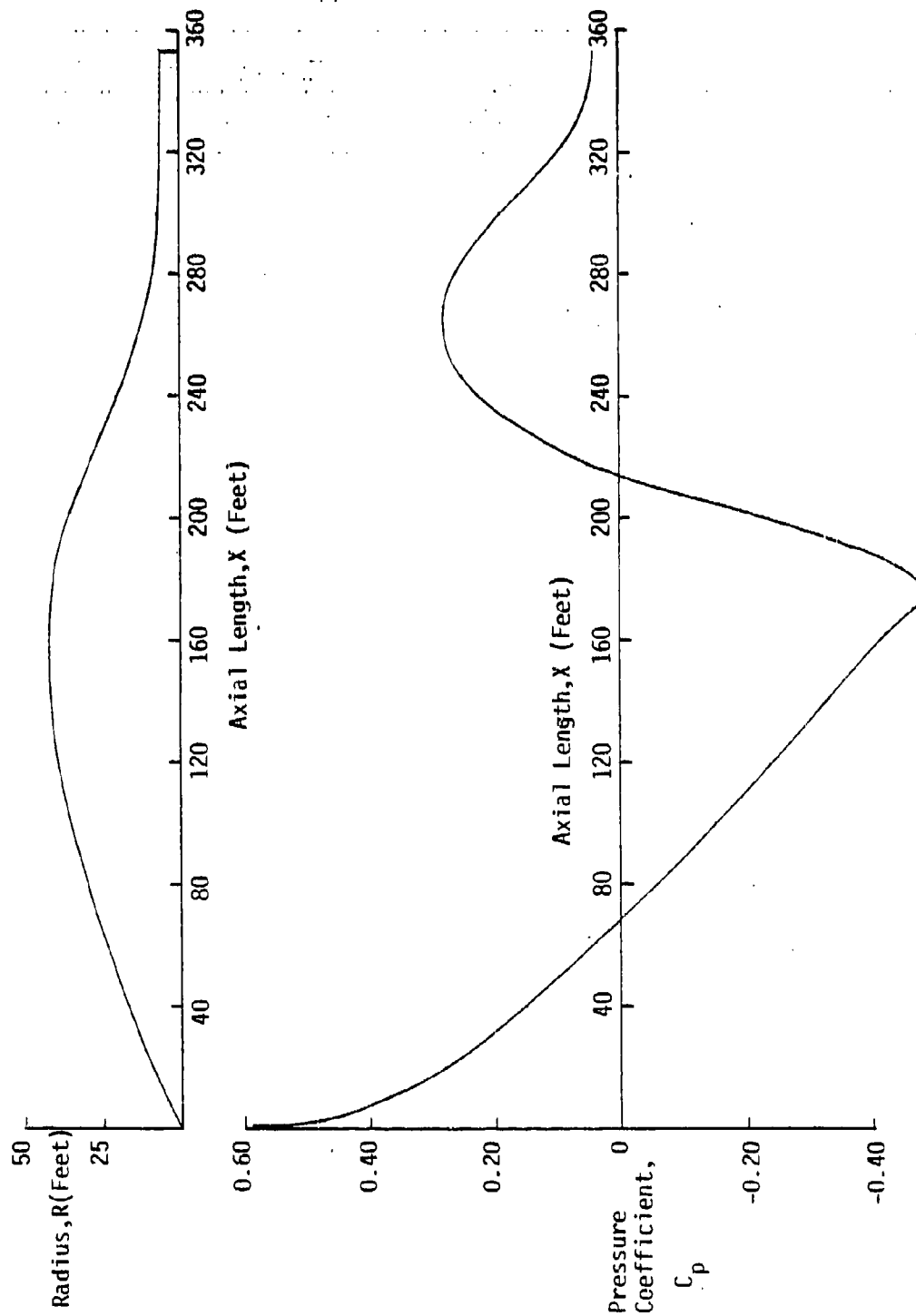


Figure 3. Geometry and Pressure Distribution of the Selected LIA Vehicle.



transition usually occurs when theoretical amplification ratios reach a level of about  $e^9$ .<sup>\*</sup> The  $e^9$  transition criterion is the most widely accepted transition prediction technique used in the laminar flow design community at the present time and has been used in this current study.

Boundary-layer stability results are presented in terms of the amplification of disturbances at particular frequencies. The term disturbance frequency, as used in the context of small disturbance linear theory, refers to the receptivity of the boundary-layer stability to disturbances of certain frequencies. Disturbance frequencies outside this range theoretically should not cause adverse effects on the laminar flow. The practical implication of this is that mechanical systems such as motors and propellers should be designed such that the vibrational frequencies of these systems fall outside the receptivity range of the boundary layer.

Boundary-layer stability results for the adiabatic LTA Vehicle are presented in Figure 4 for an altitude of 55,000 feet and a freestream speed of 80 knots. The nondimensional disturbance frequencies<sup>\*\*</sup> that are amplified range from  $\omega=0.111 \times 10^{-4}$  (31 Hz) to  $\omega=0.402 \times 10^{-4}$  (113 Hz). The frequency that shows amplification farthest upstream on the vehicle hull is  $\omega=0.402 \times 10^{-4}$ ; this amplification starts at an arc-length location of about 15 feet. The maximum amplification ratio is  $e^{7.7}$  corresponding to a disturbance frequency  $\omega=0.185 \times 10^{-4}$  (52 Hz); this occurs at an arc-length location of about 140 feet. The maximum amplification ratio for

---

\* Actually, the magnitude of the exponent represents an empirically derived averaged value based on correlations performed between theory and transition experiments. From these correlations the exponent varied from 8 to 12 with 9 being an average value.

\*\* The corresponding dimensional frequencies,  $\omega'$  are given in the parentheses. The nondimensional frequencies,  $\omega$  are defined as  $\omega=\omega'v/U_\infty^2$ .

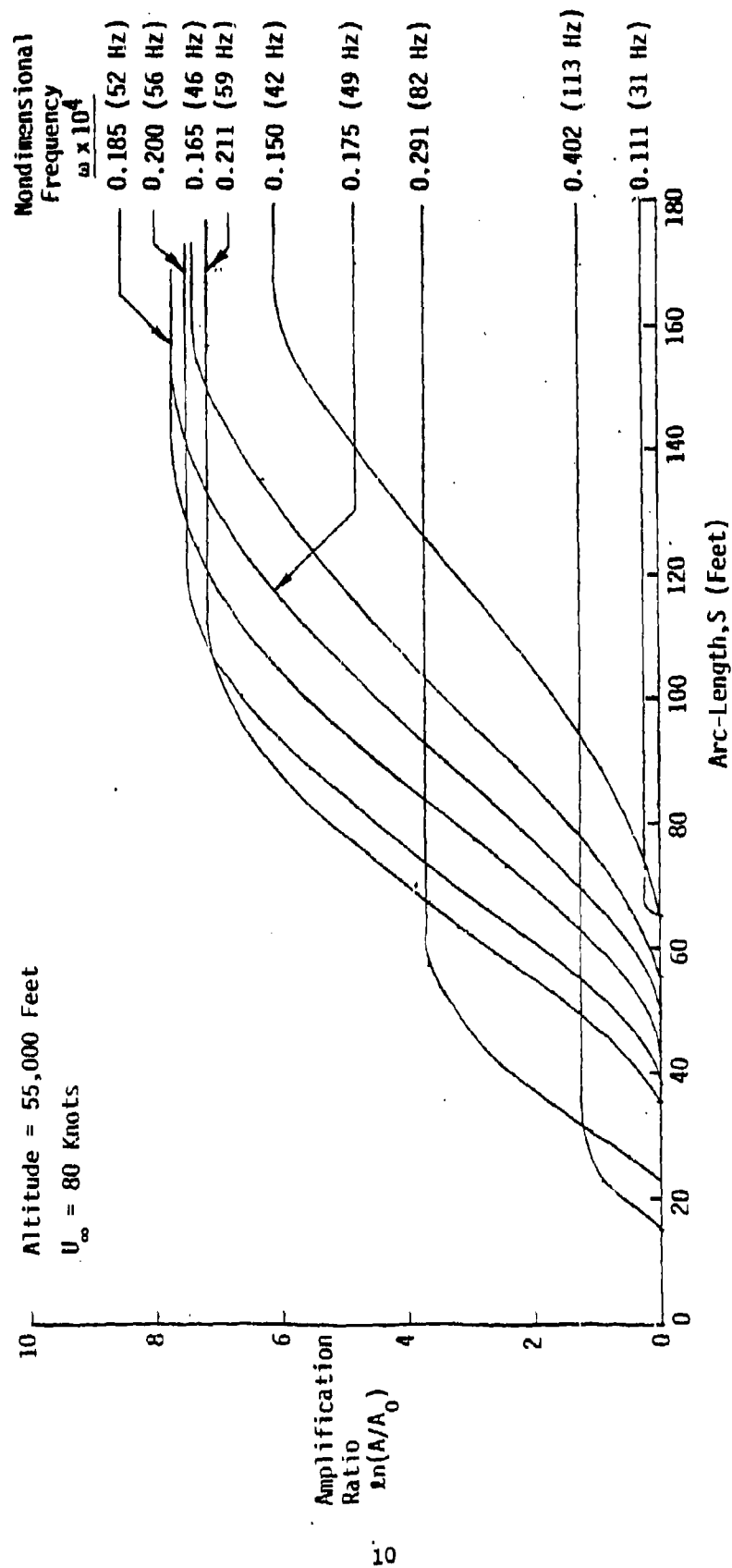


Figure 4. Boundary-Layer Stability Results for the Selected LTA Vehicle at Adiabatic Conditions.

the design condition is below the  $e^9$  transition criterion level, therefore laminar flow should be sustained to the location of laminar separation assuming adiabatic conditions on the vehicle and that the surface finish meets or is below the allowable limits,\* and neglecting any external disturbance such as freestream turbulence.

Freestream turbulence levels at the proposed operational altitudes of the LTA Vehicle were not available for this current study. The freestream turbulence levels at these altitudes are believed to be very low, and thus, their effects were neglected. If quantitative freestream turbulence data are available, their effects on vehicle laminar flow can be assessed using the  $e^n$  stability technique of Mack (1977).

---

\* These effects are addressed in Section 6.

#### 4. BOUNDARY-LAYER ANALYSIS INCLUDING SOLAR RADIATION

Part of the mission requirements for the LTA Vehicle is that the vehicle operate both day and night for a nominal 30-day period. During the daytime, the radiation from the sun will heat the surface\* of the LTA Vehicle. The equilibrium surface temperature of the vehicle will be primarily a function of the solar radiation intensity, and the material characteristics of the surface. The surface temperature of the LTA Vehicle has been estimated using a thermal equilibrium model. This model is based on a steady-state net heat-flux balance for the heated portion of the vehicle surface and consists of solar radiation absorbed by the surface,\*\* radiation emitted from the surface and forced convection associated with a laminar boundary-layer flow over the vehicle surface up to laminar separation. Other thermodynamic effects such as shell conduction, internal radiation, and upward radiation from the earth surface have been neglected in this model.

This equilibrium heat flux model is represented below in Equation 1.

$$q_{\text{net}} = q_{\text{ab}} - q_{\text{rad}} - q_{\text{con}} \quad (1)$$

---

\* The effect of surface heating, in air, on laminar flow stability was investigated by Liepmann and Fila (1947); their results showed that surface heating was destabilizing to a laminar boundary layer.

\*\* The effect of vehicle geometry has not been included in the assessment of solar radiation normal to the surface, therefore, the final equilibrium temperature will be an upper bound estimate.

where

$q_{ab}$  = Heat flux absorbed by surface;  $\alpha_s G_s$

$q_{rad}$  = Heat flux radiated from surface;  $\epsilon \sigma T^4$

$q_{con}$  = Heat flux removed from surface by forced convection;  $f(T, c_f)$

and

$T$  = Steady-state vehicle surface temperature;  $^{\circ}R$

$c_f$  = Local skin friction coefficient

$\alpha_s$  = Absorptivity of the vehicle surface material

$G_s$  = Solar radiation, 400 Btu/hr-ft<sup>2</sup>\*

$\epsilon$  = Emissivity of the blimp surface material

$\sigma$  = Stefan-Boltzmann constant;  $1.714 \times 10^{-9}$  Btu/hr-ft<sup>2</sup>- $^{\circ}R^4$

The radiation terms of  $q_{ab}$  and  $q_{rad}$  are functions of the material characteristics of the LTA Vehicle hull. The material of the hull for this heat flux analysis is assumed to be very similar to that used for weather balloons. The absorptivity of this material is  $\alpha_s = 0.196^{**}$  and its emissivity is  $\epsilon = 0.640^{**}$ .

An equilibrium temperature can be determined by prescribing a zero net heat flux in Equation 1. An iterative scheme was developed to find the

---

\* This value of solar radiation represents an estimate for an altitude of 55,000 feet based on available exo-atmospheric and earth surface data.

\*\* These material specifications were obtained from Mr. Sam Greenhalgh of NADC.

equilibrium temperature of the LTA Vehicle surface since the skin friction distribution was not known *a priori*. This iterative scheme involved performing a boundary-layer computation with an initial guess of the temperature distribution over the vehicle surface as input. The TAPS boundary-layer output provided the convective heat flux distribution over the surface. This distribution of  $q_{con}$  was then inserted into Equation 1 to check if a net heat flux of zero was established. For a resulting  $q_{net}$  different from zero, a revised estimate of the temperature distribution was made based on the trend of the earlier results and the above steps were repeated. Convergence of  $q_{net}$  to nearly zero was usually obtained within two to three iterations. The computed wall overheat distribution for the LTA Vehicle based on the equilibrium model is shown in Figure 5 for an altitude of 55,000 feet and a freestream speed of 80 knots. The surface overheat rapidly increases from zero in the nose region and approaches a value of  $T_w - T_\infty$  of about 100°F at a vehicle arc-length location of about 190 feet. This final temperature distribution which satisfied the equilibrium model was utilized to obtain the pertinent boundary-layer parameters, which were used to determine the stability of the heated laminar boundary layer.

The location of boundary-layer transition from laminar to turbulent flow for the heated LTA Vehicle was estimated using a boundary-layer shape factor<sup>†</sup> correlation with  $e^9$  stability theory. The shape factor,  $H$ , is defined as the ratio of boundary-layer displacement thickness,  $\delta^*$ , to boundary layer momentum thickness,  $\theta$ . Presented in Figure 6 is the shape factor distribution for the LTA Vehicle that resulted from the equilibrium temperature distribution input to the TAPS boundary-layer

---

† The boundary-layer velocity and temperature profiles for the heated LTA Vehicle were altered to such a degree that the profiles were beyond the analysis range of the TAPS stability code. Consequently, the  $e^9$  stability technique for estimating the location of boundary-layer transition could not be utilized for this heated case.

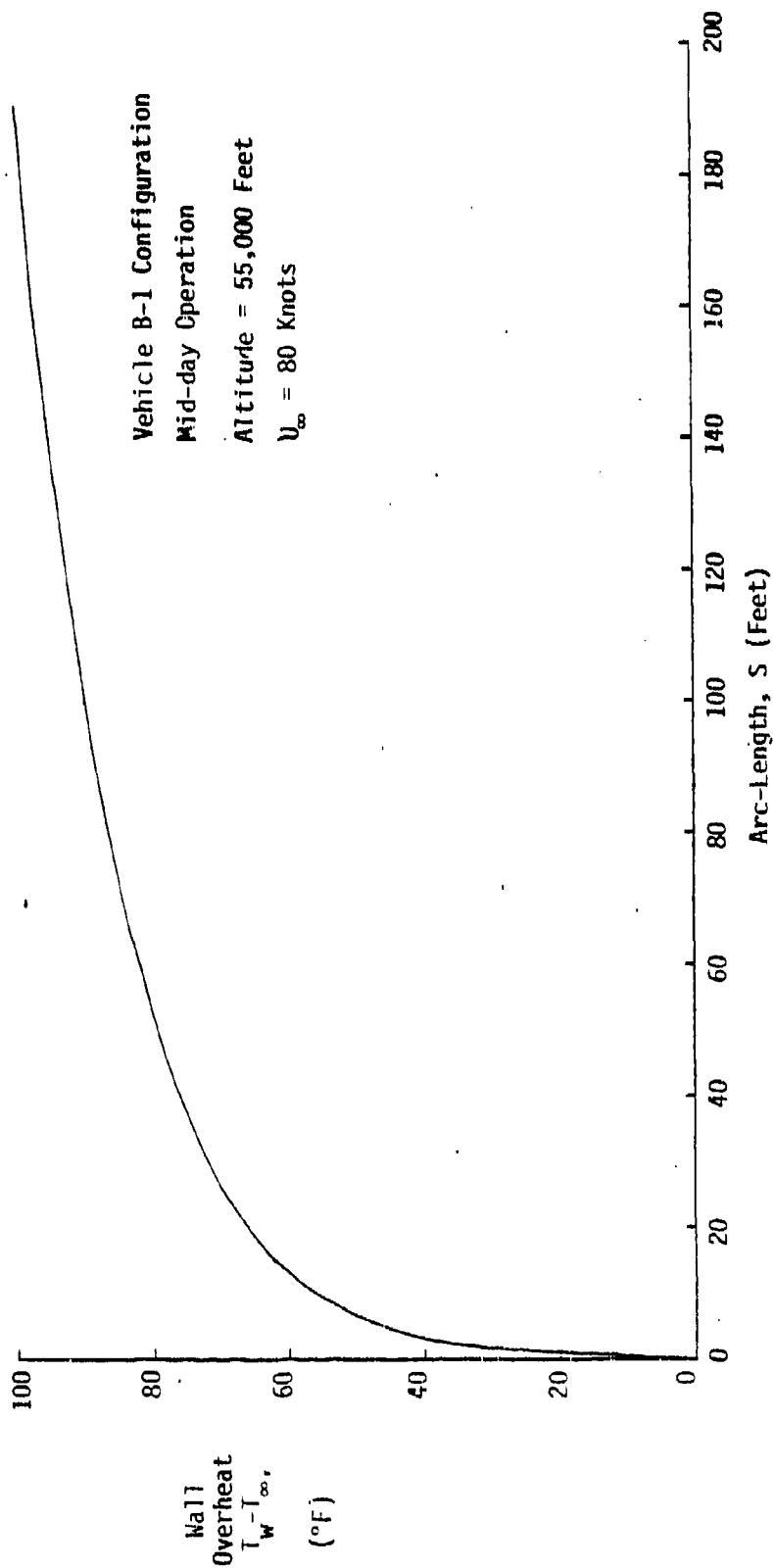


Figure 5. Equilibrium Surface Temperature Distribution for the LTA Vehicle.

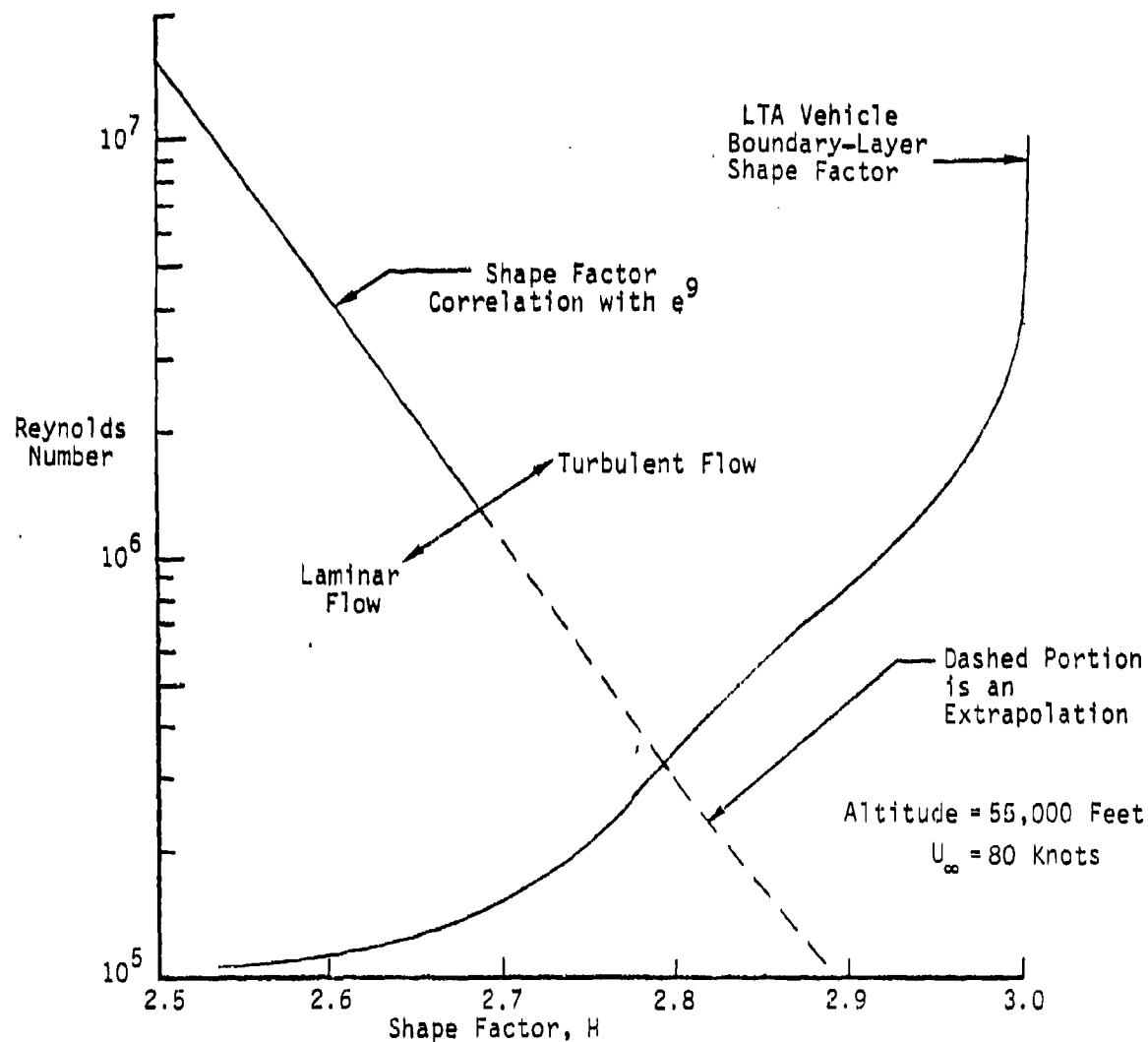


Figure 6. Boundary-Layer Shape Factor Variation for the LTA Vehicle Including Effects of Solar Radiation.



code. Also presented in Figure 6 is a curve which represents a correlation of shape factor as a function of arc-length Reynolds number that yields spatial amplification ratios of  $e^9$  (Smith, Wazzan and Hsu, 1977). The intersection of these two curves indicates the value of the shape factor at which the amplification ratio of small disturbances should reach  $e^9$ ; this occurs at a shape factor value of approximately 2.8. The dashed portion of the shape factor correlation curve is an extrapolation of the correlation to lower Reynolds numbers, therefore to provide a conservative transition criterion, a shape factor of 2.9 was used to determine the transition location in the heated region of the forebody hull. The shape factor of 2.9 at the design conditions corresponds to an arc-length transition location of about 21 feet aft of the vehicle nose in the heated region. This turbulent region induced by surface heating is restricted to the portion of the vehicle surface exposed to solar radiation.

An end view schematic of the vehicle hull showing the incoming solar radiation is shown in Figure 7; in this figure the angle  $\beta$  is the included angle of the turbulent region resulting from surface heating. Note that the solar radiation normal to the surface decreases as a function of  $\cos(\beta/2)$ .

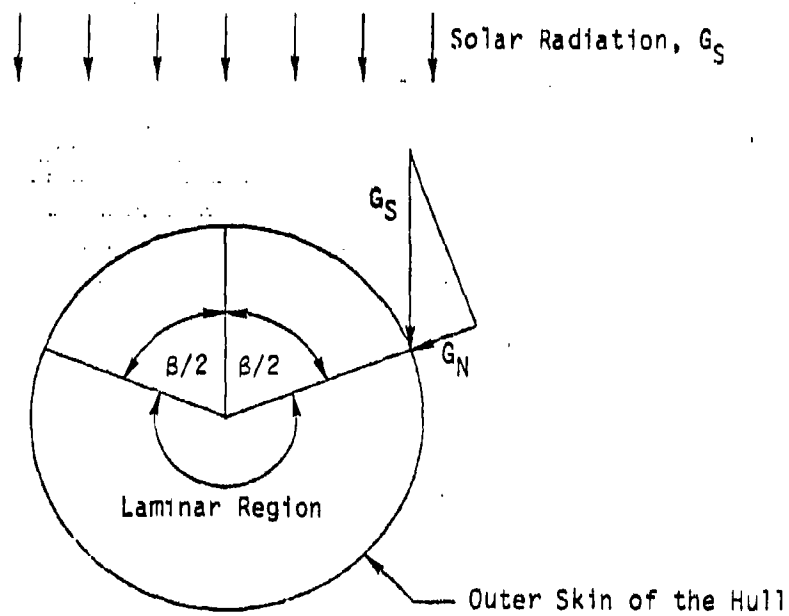


Figure 7. End View Schematic of Vehicle Showing Turbulent and Laminar Flow Regions.

## 5. LTA VEHICLE DRAG ESTIMATES

The vehicle drag estimates presented in this section include contributions from hull drag (utilizing an existing laminar flow configuration), fin drag, gondola drag, and interference and support wire drag. Total drag coefficients for the LTA Vehicle are presented for several flow conditions over the vehicle surface and, in addition, shaft horsepower comparisons are made between the nominal daytime estimated drag of the LTA Vehicle and the previous HI-SPOT drag estimates of Marcy and Hookway (1979).

### 5.1 Hull Drag Estimates

Hull drag estimates have been made for three separate boundary-layer flow conditions. These three conditions include laminar flow over the entire forebody up to the location of laminar separation (arc-length of 195 feet), turbulent flow over the entire vehicle hull, and a mixed flow condition which provides what is termed a nominal daytime hull drag estimate. This last flow condition accounts for the destabilizing influence of solar heating of the LTA Vehicle surface and the associated drag increase of the hull as a result of laminar flow breakdown in the heated region. The first two flow conditions represent lower and upper bound drag estimates for the LTA Vehicle hull. The local skin friction coefficients from these two flow conditions are utilized in determining the hull drag for the third nominal daytime flow condition (see Appendix A).

The nominal daytime flow condition considered in this section for drag analysis consists of an assumed turbulent region with an included angle,  $\beta$  of 120 degrees. The normal heat flux into the vehicle surface for  $\beta/2$  equal to 60 degrees is one half of that of the incoming normal solar radiation and decreases rapidly for  $\beta/2 > 60$  degrees.\* In addition to the turbulent region resulting from surface heating, an additional turbulent area, resulting from turbulent spreading, must be considered. A two-dimensional schematic of the turbulent area resulting from surface heating and turbulent spreading angles,  $\theta$  of 10 degrees\*\* are presented in Figure 8.

The total drag coefficient for the LTA Vehicle hull including the effects of solar radiation is obtained from Equation 2,

$$C_D = \frac{D_L + D_t}{1/2 \rho_\infty U_\infty^2 V^{2/3}} ; \quad (2)$$

where  $D_L$  is the hull drag contribution resulting from the region of laminar flow, and  $D_t$  is the hull drag contribution resulting from the turbulent flow region. The corresponding units for the terms in Equation 2 are  $D_L$  and  $D_t$  in lbs,  $\rho_\infty$  in slugs per cubic feet,  $U_\infty$  in feet per second, and  $V^{2/3}$  ( $V$  = volume) in square feet. Additional details related to the determination of  $D_L$  and  $D_t$  are presented in Appendix A. The hull drag results for the three specified flow conditions are presented in Table 1, for a relative vehicle speed of 80 knots.

---

\* The value of  $\beta$  equal to 120 degrees is an estimate only of the included angle for the turbulent flow region. This value is believed to be reasonable for performing representative vehicle drag calculations during daytime operation. This estimate should be refined further in future studies (see recommendations in Section 7).

\*\* The included turbulent spreading angle of a turbulent wedge has been measured on an axisymmetric body to be about 20 degrees (Warner and Haigh, 1978).

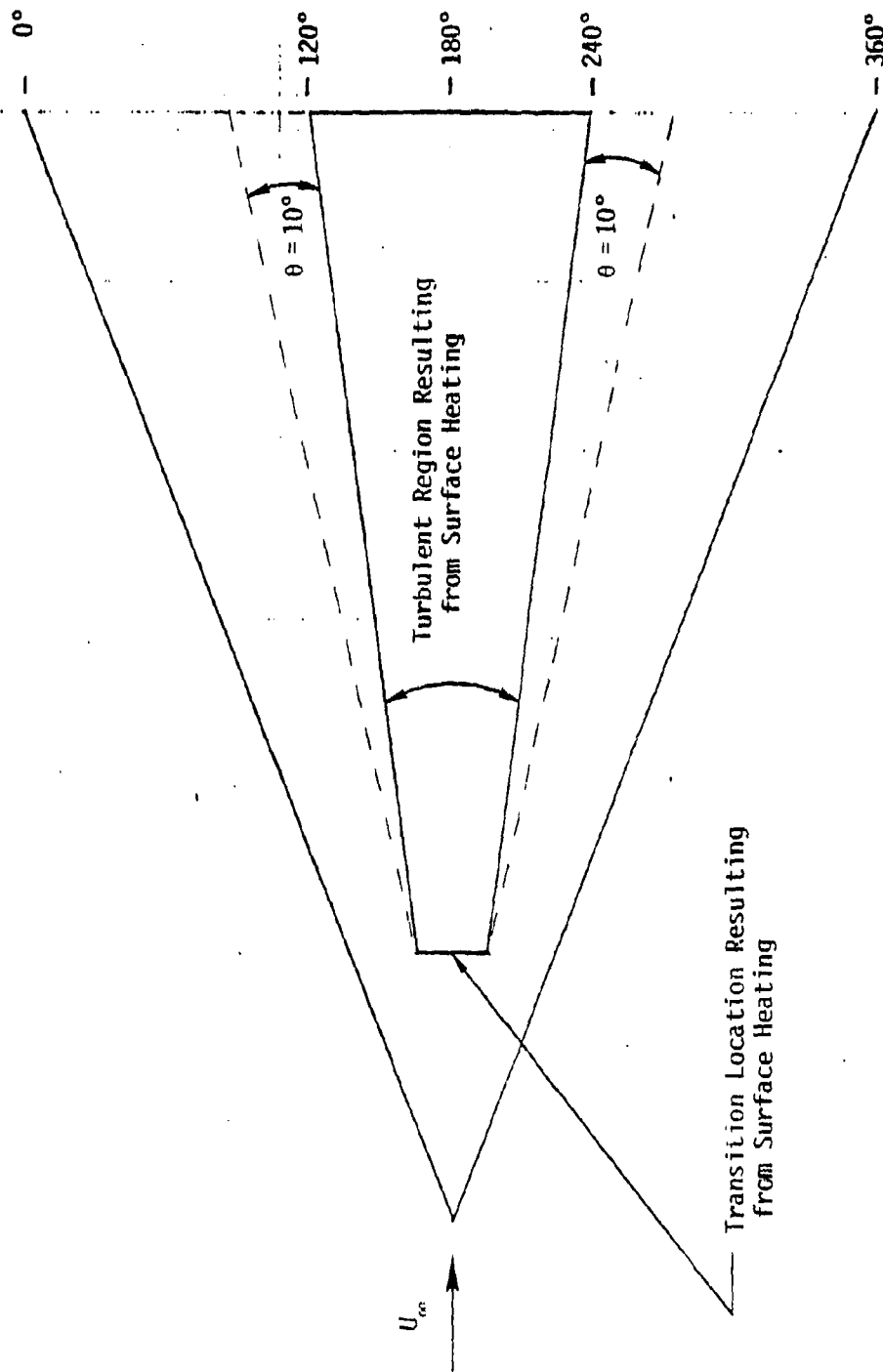


Figure 8. Schematic of the Vehicle Showing Geometry of Turbulent Flow.

Table 1. Hull Drag Estimates for Specified Flow Conditions

$C_D^*$	Drag (lb)	Flow Conditions
0.00642	144.7	Laminar flow to laminar separation (nighttime)
0.01084	244.3	Nominal daytime estimate of hull drag
0.01770	399.1	Turbulent flow

5.2 Fin Drag Estimates

Fin drag estimates have been made for the two fin geometries presented in Figure 9. The first configuration, fin 1, represents the fin geometry for the HI-SPOT Vehicle. The proposed stabilizing fins for the HI-SPOT Vehicle consist of three fins each having a wetted area of 1813 ft<sup>2</sup>. The second configuration, fin 2, represents a laminar flow fin\*\* currently used on a laminar flow submersible (Vehicle B-1) scaled up to the LTA Vehicle size. The laminar flow fin configuration consists of four fins each having a wetted area of 1038 ft<sup>2</sup>.

The drag of the fin 1 configuration consists of skin friction drag for an assumed boundary-layer transition location corresponding to an arc-length Reynolds number of about  $5 \times 10^5$ . The drag of the fin 2 configuration consists of skin friction drag for boundary-layer transition occurring at an arc-length Reynolds number of about  $1.38 \times 10^6$ , which is

---

\* The drag coefficient is based on a reference area of hull volume to the 2/3 power.

\*\* Laminar flow fins will probably have a weight penalty relative to HI-SPOT type fins since surface rigidity must be maintained for laminar flow.

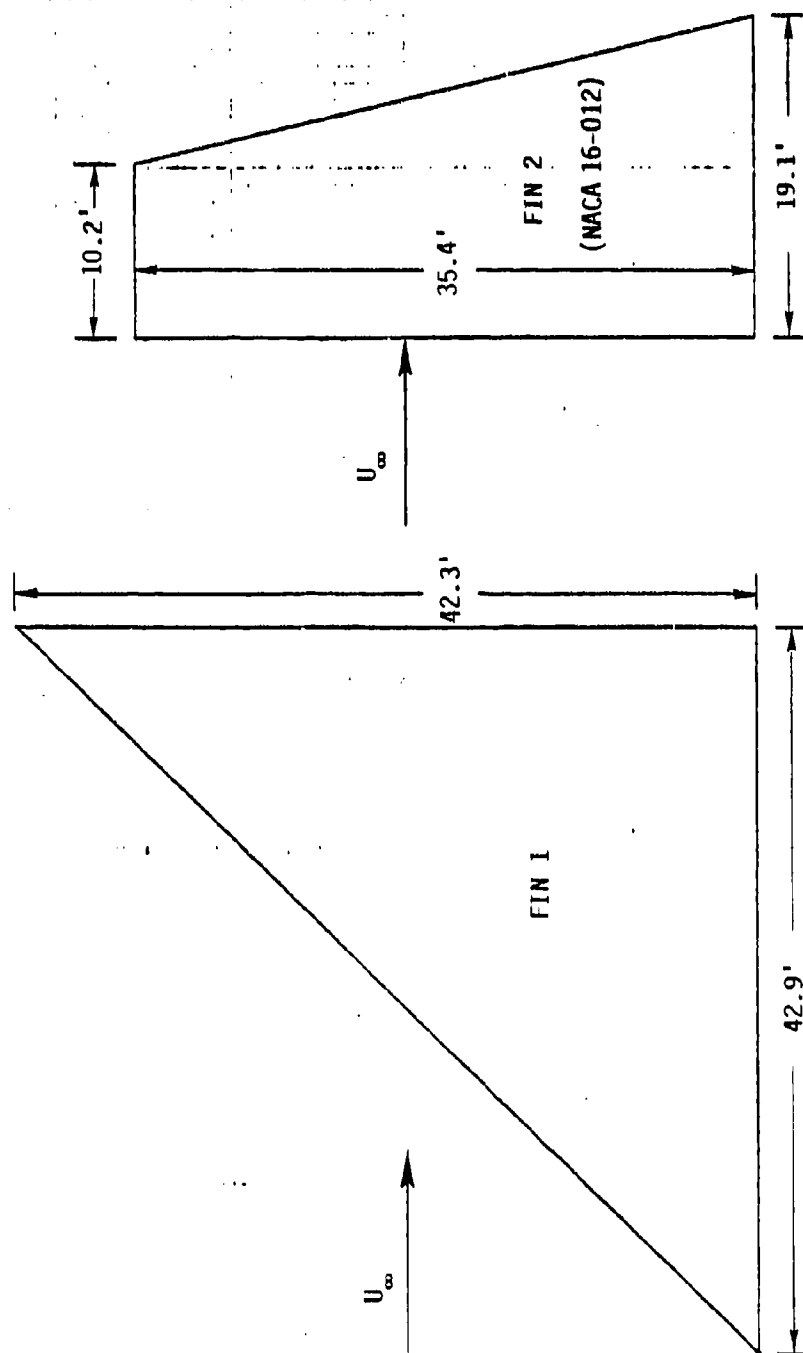


Figure 9. Control Fin Configurations for the LIA Vehicle.

based on the minimum pressure location on the NACA 16-012 airfoil section. The fin drag results for the two fin configurations are presented in Table 2 for a freestream speed of 80 knots and an altitude of 55,000 feet.

Table 2. Fin Drag Estimates for Two Fin Configurations

$C_D^*$	Drag (lb)	Fin Type
0.001946	43.9	Fin 1 configuration (3 fins)
0.000864	19.5	Fin 2 configuration (4 fins)

### 5.3 Gondola Drag Estimates

It is assumed in this study that the required LTA Vehicle payload and propulsion powerplant are carried in a gondola. Alternate powerplant locations were considered in Marcy and Hookway (1979), but according to their study the gondola location is preferred since this reduces structural complexities by placing the concentrated weight of the powerplant close to the LTA Vehicle center of gravity.

The propeller diameter for the HI-SPOT Vehicle is about 23 feet, however this is based on an optimistic vehicle drag estimate at a speed of 80 knots (as vehicle drag increases, propeller diameter usually increases), therefore, for gondola sizing a propeller diameter of 25 feet is assumed. Presented in Figure 10 is a schematic of the gondola-hull junction for a propeller diameter of 25 feet. The gondola size is basically a function of propeller diameter and required width. The HASPA

---

\* The drag coefficient is based on a reference area of hull volume to the 2/3 power.



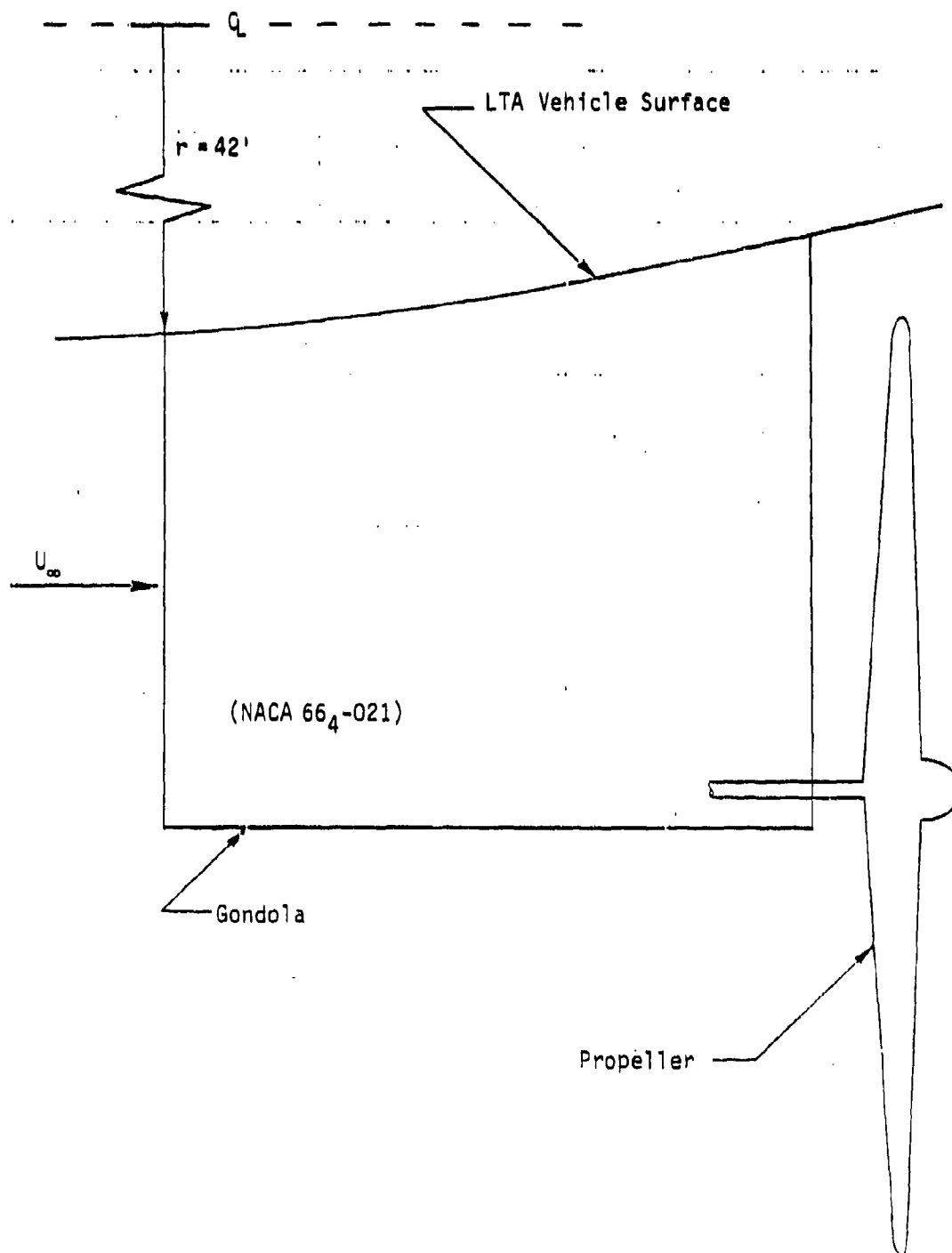


Figure 10. Schematic of the Gondola-Hull Junction.

gondola (Scales and McComas, 1977), consisted of a width of about 3.5 feet, which will be utilized for this current study to size the gondola for the LTA Vehicle. The gondola shown in Figure 10 has a chord length of 16.7 feet, an average depth of about 14 feet, and a width of 3.5 feet. The airfoil section selected for the gondola consists of a NACA 66<sub>4</sub>-021 section.

The drag of this gondola has been estimated using two independent approaches. The first is based on data presented in Hoerner (1965) for gondola shapes and the second is based on the section drag coefficients for the NACA 66<sub>4</sub>-021 airfoil section, Abbott and Doenhoff (1959). Information presented in Hoerner shows that the gondola drag coefficient for an aerodynamically clean configuration (based on gondola frontal area) is about 0.1.\* The section drag coefficient (based on planform area) for the NACA 66<sub>4</sub>-021 airfoil section is about 0.0055 for a gondola chord Reynolds number of about  $2.2 \times 10^6$ . The gondola drag results are presented in Table 3 for a freestream speed of 80 knots and an altitude of 55,000 feet for both calculational approaches.

---

\* Results in Hoerner show gondola drag coefficients as high as 0.6 but these values are for non-streamlined aerodynamic configurations.

Table 3. Gondola Drag Estimates

$C_D^*$	Drag (lb)	Comments
0.000792	17.9	Hoerner estimate for aerodynamically clean configuration.
0.000160	3.6	Estimate from Abbott and Doenhoff, NACA 66 <sub>4</sub> -021 airfoil.

The substantial difference in these two gondola drag estimates is believed to be primarily a result of Hoerner's estimate including interference drag, whereas the airfoil data does not include this effect. These differences are not significant to the total vehicle drag estimates, since the gondola drag is a small percentage of the total vehicle drag (see results in Table 4 of Section 5.5).

#### 5.4 Interference and Support Wire Drag Estimates

The interference drag of subsonic, propeller-driven airplanes is usually assumed to be about 5 percent of the wetted area drag of the airplane (Roskam, 1971). The interference drag of the LTA Vehicle is probably less than the standard 5 percent factor (3 percent to 4 percent factor is probably representative) since the ratio of interference area\*\* divided by total surface area is less for the LTA Vehicle than it is for a standard propeller-driven airplane.

---

\* The drag coefficient is based on a reference area of hull volume to the 2/3 power.

\*\* The interference area is the summation of the intersection areas of wings and appendages on the fuselage or hull.

Details of wire support and suspension structures were not available for this study, but information presented in Scales and McComas (1977) suggest that the support wire drag is about 1 percent of the total skin friction drag of the vehicle. Therefore, a factor of 5 percent that accounts for both interference drag and support wire drag will be used in making total drag estimates for the LTA Vehicle.

### 5.5 Total Drag Estimates for the LTA Vehicle

The total drag estimates for the LTA Vehicle consist of a summation of the drag of the various components documented in Section 5.1 through 5.4. Low, high, and nominal daytime estimates of the total drag values for the LTA Vehicle are presented in Table 4 for a freestream speed of 80 knots and an altitude of 55,000 feet.

Table 4. LTA Vehicle Total Drag Estimates

$C_D^*$	Drag (lb)	Comments
0.0078	176.	Low Drag Estimate: laminar flow to laminar separation on hull, laminar flow fins (fin 2) and low drag gondola.
0.0136	306.	Nominal Daytime Drag Estimate: hull viscous drag includes solar heating effects, turbulent flow fins (fin 1), and low drag gondola.
0.0215	484.	High Drag Estimate: hull viscous drag turbulent, turbulent flow fins (fin 1), and turbulent flow gondola.

\* The drag coefficient is based on a reference area of hull volume to the 2/3 power.

The estimated shaft horsepower requirements for the LTA and HI-SPOT Vehicles are 89 hp and 50 hp, respectively, for a propulsion efficiency,  $\eta_p$  of 0.85. These shaft horsepower levels are based on an operational altitude of 55,000 feet and a freestream speed of 80 knots. The shaft horsepower requirement for the LTA Vehicle is based on the nominal daytime drag estimate while the shaft horsepower estimate for the HI-SPOT Vehicle was obtained from Marcy and Hookway (1979). The estimated shaft horsepower for the HI-SPOT Vehicle is very optimistic; for example, a shaft horsepower of about 50 hp is required for the LTA Vehicle if the forebody of the hull is completely laminar (no destabilized regions resulting from solar radiation) and if laminar flow fins and a low drag gondola are utilized.

Reductions in the estimated shaft horsepower for the LTA Vehicle could probably be attained if a parametric design study was performed utilizing low drag technology for the vehicle fins and gondola. However, values as low as 50 SHP would not be obtained for a passive stabilized hull based on the surface heating results presented in Section 4. It is important to note, that even with the results of solar radiation accounted for, a considerable reduction in shaft horsepower can be attained relative to a turbulent hull configuration. The required shaft horsepower for a turbulent hull with a propulsion efficiency of 0.85 ranges between 129 hp to 140 hp depending on the fin and gondola configurations, whereas the shaft horsepower for the daytime operation of the LTA Vehicle is only 89 hp.

## 6. VEHICLE DESIGN CONSIDERATIONS

There are several practical constraints to consider in the design of a laminar flow LTA Vehicle. The vehicle skin must be sufficiently rigid and the surface finish must meet certain allowable roughness and waviness criteria. In addition, support cables and external structures should not be used in the laminar flow portion of the hull.

The allowable roughness height as a function of vehicle arc-length can be estimated based on a conservative roughness Reynolds number criterion established by Smith and Clutter (1957). This criterion consists of correlations between transition experiments involving roughness elements and theoretical calculations of a roughness Reynolds number based on these experimental data. The relevant roughness Reynolds number is defined as

$$Re_k = \frac{u_k k}{\nu_k} \quad (3)$$

where:

$k$  is the height of the roughness element

$u_k$  is the fluid speed at the top of the roughness element

and

$\nu_k$  is the kinematic viscosity at the height  $k$

The results of the Smith and Clutter correlation of Equation 3 with experimental data have shown that if  $Re_k \leq 25$ , laminar flow is not affected by the roughness element(s). The allowable roughness heights for the adiabatic and heated LTA Vehicle are presented in Figure 11 as a function of vehicle arc-length. The allowable roughness heights for the heated boundary layer range from about 20 mils in the nose region to about 45 mils at a vehicle arc-length of 175 feet. The corresponding allowable roughness heights for the adiabatic boundary layer range from about 18 mils to 35 mils. Therefore, if the rms surface finish is maintained at or below these allowable roughness heights, distributed roughness over the vehicle skin will not affect the laminar flow.

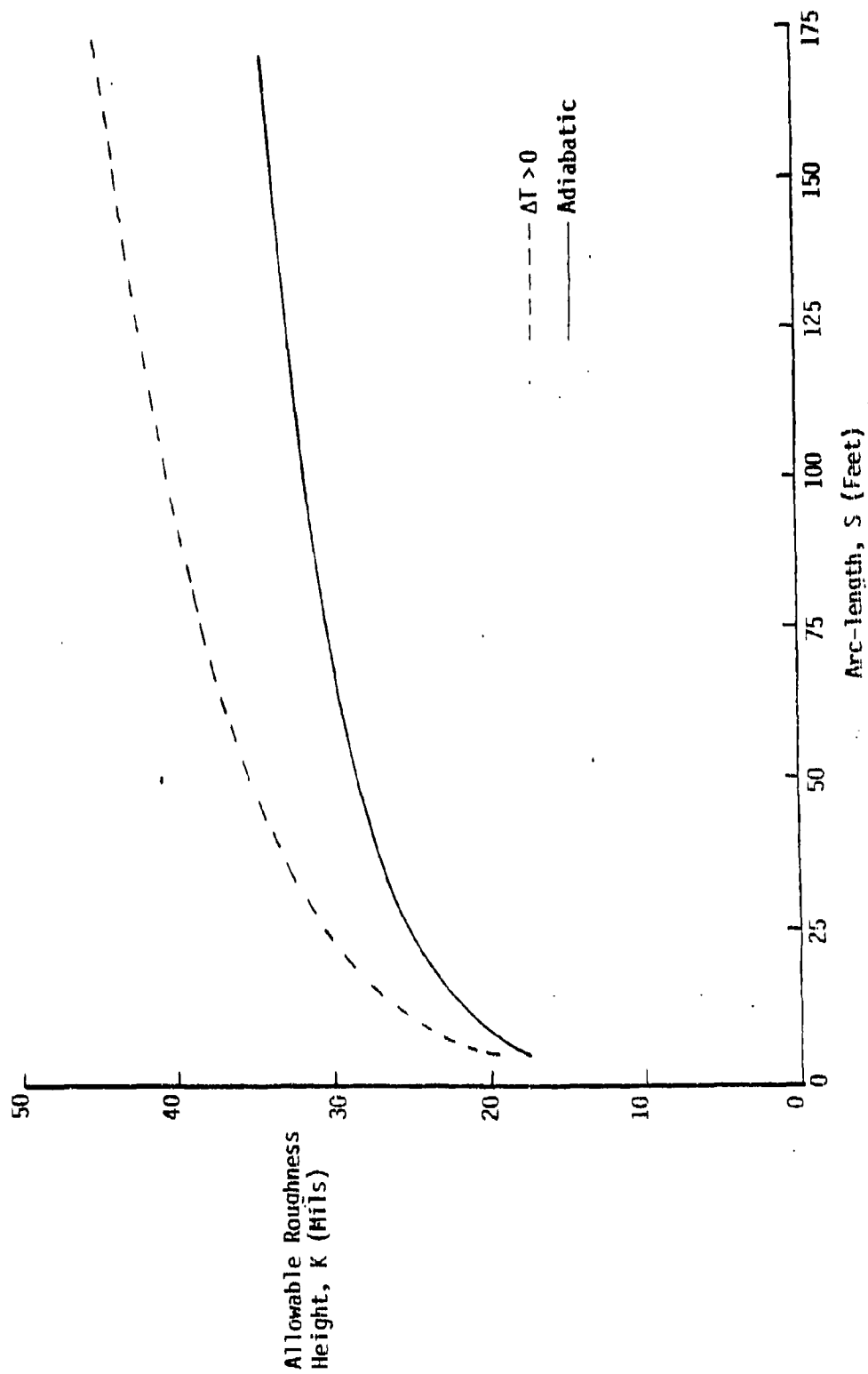


Figure 11. Allowable Roughness Height for the LIA Vehicle.

The surface waviness criterion that has been applied to the present LTA Vehicle is based on a data correlation by Carmichael (1959). This criterion is presented in Equation 4, and has been cautiously used in the design of laminar flow submersibles.

$$\frac{h}{\lambda} = \left[ \frac{59000 c}{\lambda (R_c)^{3/2}} \right]^{1/2} \quad (4)$$

In this formulation,  $h$  is the allowable wave amplitude for a given wavelength,  $\lambda$ ,  $c$  is the wing chord, and  $R_c$  is the chord Reynolds number. This correlation was obtained from waves placed on laminar flow wings. The boundary-layer flow on these wings was stabilized using boundary-layer control by suction with laminar flow obtained over the full chord. A critical wave was defined as the minimum size wave which prevented the attainment of laminar flow to the trailing edge with moderate suction levels. Since  $c$  in this expression represents the maximum length of laminar flow, for the present purposes  $c$  is interpreted to represent the arc-length from the nose of the vehicle to the laminar separation location.

The allowable surface waviness heights for the LTA Vehicle at a vehicle speed of 80 knots and an altitude of 55,000 feet, are 33 mils for a  $\lambda$  of 1 inch and 114 mils for a  $\lambda$  of 1 foot. The allowable surface waviness heights as obtained from Equation (4) are independent of location on the body surface. In general, it is believed that allowable waviness heights should be a function of location on the vehicle surface. This factor, together with the limited test parameter variations in the previous tests, demonstrates the need for additional effort in this waviness criterion area.\*

---

\* An experimental investigation of laminar flow breakdown resulting from surface waviness on an axisymmetric body is currently being planned at the Naval Ocean Systems Center (Ladd, 1980). The results from this experiment, when available, should be reviewed and compared with Equation (4) since this data correlation was developed from limited transition test data.



In summary, the LTA Vehicle design should meet the following specifications in order to ensure that laminar flow is maintained on the forebody hull:

- Support wires and external structures should be placed in the turbulent flow region on the vehicle.
- The surface skin should be rigid and should not flutter or vibrate during operation.
- The rms surface roughness height should not exceed 18 mils in the nose region.
- Surface waviness heights should not exceed 33 mils for a 1 inch wavelength and 114 mils for a 1 foot wavelength.

## 7. SUMMARY AND RECOMMENDATIONS

The feasibility of applying laminar boundary-layer control to an LTA Vehicle has been assessed including the effect of solar radiation on the laminar flow. The investigation of the effect of solar-radiation-induced surface heating on the stability of the laminar flow has shown that surface heating is destabilizing and causes the laminar flow to break down on regions of the vehicle surface exposed to high levels of solar radiation. Aerodynamic drag estimates for the LTA Vehicle, including the effects of solar radiation, have shown that a substantial reduction in drag can be achieved relative to a conventional turbulent configuration. A realistic drag reduction factor of about 1.6 can be obtained with a laminar flow LTA Vehicle during daytime operation, with the factor approaching 2.4 during night operations.

This current study has addressed the feasibility of maintaining laminar flow on an LTA Vehicle, using a laminar flow submersible configuration (Vehicle B-1) for this assessment. This particular vehicle design, however, is not necessarily the optimal configuration for the LTA Vehicle mission since optimal design configuration studies were not part of this investigation.

The practical difficulties associated with utilizing laminar flow control on the high altitude LTA Vehicle have been investigated. These results show that, if the surface waviness and roughness criteria can be satisfied for this application, a laminar flow LTA Vehicle can be designed. Recommendations which will lead to a firmer technical foundation for the application of laminar flow control to a high altitude LTA Vehicle are presented below:

- Refine the solar radiation model accounting for heat flux variations as a function of vehicle geometry, and reassess the boundary-layer flow over the vehicle.

- Perform optimal design configuration studies for the hull using existing inverse design methods (i.e., computations of vehicle geometries corresponding to selected pressure distributions).
- Perform vehicle endurance calculations based on vehicle drag estimates for both day and night operations and wind speed variations throughout the year.
- Review current waviness criteria and their application to the LTA Vehicle mission and also investigate surface waviness which could result from aerodynamic loading of the LTA Vehicle skin.
- Perform a coupled analysis of the heat destabilized region investigating the possibility of re-laminarization since turbulent boundary-layer flow will reduce the vehicle surface over-heat by a factor between 5 and 7.
- Review state-of-the-art materials and coatings such as those used in space-craft operations to minimize the  $\alpha_s/\epsilon$  ratio of the exposed surface.
- Investigate complementary concepts for reducing vehicle drag such as an integrated propulsion and vehicle control system which would allow the removal of the vehicle fins or a reduction in their size.

## 8. REFERENCES

- Abbott, I.H. and von Doenhoff, A.E. (1959), Theory of Wing Sections, Dover Publications, Inc., New York.
- Carmichael, B.H. (1959), "*Surface Waviness Criteria for Swept and Un-swept Laminar Suction Wings*," NORAIR Report No. NOR-59-438 (BLC-123), August.
- Gentry, A.E. and Wazzan, A.R. (1976), "*The Transition Analysis Program System, Volume II - Program Formulation and Listing*," McDonnell Douglas Report No. MDC J7255/02, June.
- Greenhalgh, S. (1980), Personal Communication, Naval Air Development Center, Warminster, Pennsylvania.
- Hoerner, S.F. (1965), Fluid-Dynamic Drag, Hoerner Fluid Dynamics, Brick Town, New Jersey.
- Jaffe, N.A., Okamura, T.T. and Smith, A.M.O. (1970), "*Determination of Spatial Amplification Factors and Their Application to Predating Transition*," AIAA Journal, Vol. 8, No. 2, January.
- Ladd, D.M. (1980), Personal Communication, Advanced Concepts Division of Naval Ocean Systems Center, San Diego, California.
- Liepmann, H.W. and Fila, G.H. (1947), "*Investigations of Effects of Surface Temperature and Single Roughness Elements on Boundary-Layer Transition*," NACA TN 1196 and NACA Report 890.
- Mack, L.M. (1977), "*Transition and Laminar Instability*," JPL Publication 77-15.
- Marcy, W.L. and Hookway, R.O. (1979), "*Propulsion Options for the HI-SPOT Long Endurance Drone Airship*," Martin Marietta Corp. Report MCR 79-632, September.
- Roskam, J. (1971), Methods for Estimating Drag Polars of Subsonic Airplanes, Roskam Aviation and Engineering Corp., Lawrence, Kansas.
- Scales, S.H. and McComas, C.B. (1977), "*High Altitude Superpressured Powered Aerostat (HASPA) Demonstration Program*," Martin Marietta Corp. Report MCR 77-435, September.

REFERENCES (Continued)

- Smith, A.M.O. and Clutter, D.W. (1957), "*The Smallest Height of Roughness Capable of Affecting Boundary Layer Transition in Low-Speed Flow*," Douglas Aircraft Report No. ES26803, August.
- Smith, A.M.O. and Gamberoni, N. (1956), "*Transition, Pressure Gradient, and Stability Theory*," Proc. Int. Congr. Appl. Mech., 9th, Brussels, Belgium 4,234.
- Smith, A.M.O., Wazzan, A.R. and Hsu, W.C. (1977), "*Laminarisation of Bodies of Revolution Moving in Water*," University of California, Los Angeles School of Engineering and Applied Science, October.
- Warner, D.J. and Haigh, W.W. (1978), "*AEMT Vehicle Wind Tunnel Test Results*," Dynamics Technology Report No. DT-7912-1, December.

APPENDIX A. MIXED FLOW DRAG ANALYSIS METHOD

The skin friction drag of an axisymmetric vehicle can be obtained by the integration of the local skin friction coefficient,  $c_f$  over the vehicle surface. Presented in Figure A1 is an end view of an axisymmetric vehicle showing turbulent and laminar flow regions (confined within the angular regions  $\beta$  and  $\alpha$ , respectively) corresponding to a region of heat destabilized flow on the LTA Vehicle. Information presented in Section 4 showed that the turbulent region spreads laterally with distance aft, therefore, the angles  $\alpha$  and  $\beta$  are functions of the vehicle arc-length. The drag equation for the laminar flow portion of the vehicle is presented in Equation A1.

$$D_L = \frac{1}{2} \rho_\infty u_\infty^2 A_{ref} C_{FL} \quad ; \quad (A1)$$

In this equation the total skin friction coefficient is

$$C_{FL} = \frac{1}{A_{ref}} \int_0^{L_S} \int_{\theta_i}^{\theta_f} c_{fL} r_o \left( \frac{u_e}{u_\infty} \right)^2 d\theta ds \quad (A2)$$

and

- $\theta_i$  is the starting angle of the laminar flow region (radians)
- $\theta_f$  is the finishing angle of the laminar flow region (radians)
- $c_{fL}$  is the local laminar skin friction coefficient
- $r_o$  is the local body radius (feet)
- $u_e$  is the edge velocity of the boundary layer (feet per second)
- $u_\infty$  is the freestream speed (feet per second)
- $A_{ref}$  is the reference area, usually vehicle volume to the 2/3 power (square feet)
- $\rho_\infty$  is the fluid density (slugs per cubic feet).

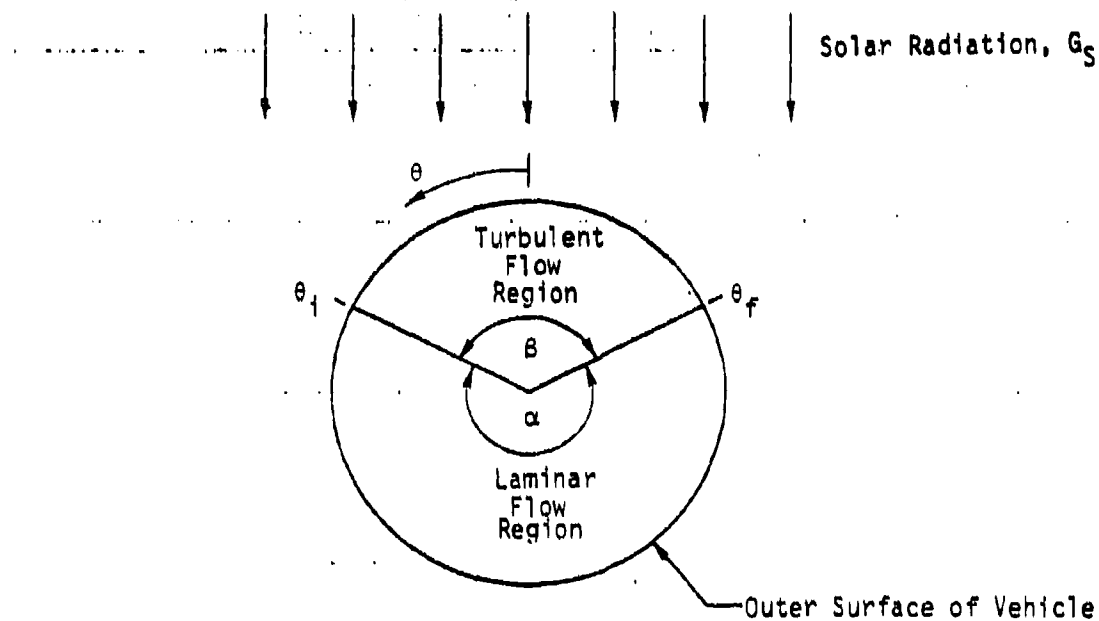


Figure A1. End View Schematic of Vehicle Hull Showing Laminar and Turbulent Flow Regions.

Integration of the  $\theta$  integral of Equation A2 yields:

$$C_{F_L} = \frac{1}{A_{ref}} \int_0^{L_S} (\theta_f - \theta_i) c_{f_L} r_o \left( \frac{u_e}{u_\infty} \right)^2 dS. \quad (A3)$$

Since  $\alpha$  is the included angle of the laminar region, i.e.,  $\alpha = \theta_f - \theta_i$ , then  $C_{F_L}$  can be written as shown in Equation (A4).

$$C_{F_L} = \frac{1}{A_{ref}} \int_0^{L_S} \alpha c_{f_L} r_o \left( \frac{u_e}{u_\infty} \right)^2 dS \quad (A4)$$

Likewise,  $C_{F_t}$  (the total turbulent skin friction coefficient) can be written as,

$$C_{F_t} = \frac{1}{A_{ref}} \int_{t_r}^{t_e} \beta c_{f_t} r_o \left( \frac{u_e}{u_\infty} \right)^2 dS, \quad (A5)$$

where  $t_e$  and  $t_r$  are the arc-length locations associated with the trailing edge of the vehicle and the boundary-layer transition location, respectively.

The skin friction drag from the laminar turbulent regions are then

$$D_L = q_\infty A_{ref} C_{F_L} = q_\infty \int_0^{L_S} \alpha (c_{f_L}) r_o \left( \frac{u_e}{u_\infty} \right)^2 dS \quad (A6)$$

and

$$D_t = q_\infty A_{ref} C_{F_t} = q_\infty \int_{t_r}^{t_e} \beta (c_{f_t}) r_o \left( \frac{u_e}{u_\infty} \right)^2 dS \quad (A7)$$

where

$$q_\infty = \frac{1}{2} \rho_\infty u_\infty^2$$



The total drag of the vehicle is  $D_l + D_t$ , and substituting  $2\pi - \alpha$  for  $\beta$  the total drag can be written as

$$D_{total} = q_{\infty} \left\{ 2\pi \int_0^{tr} (c_{f_l}) r_o \left( \frac{u_e}{u_{\infty}} \right)^2 dS + 2\pi \int_{tr}^{ls} (c_{f_t}) r_o \left( \frac{u_e}{u_{\infty}} \right)^2 dS + \right. \\ \left. - \int_{tr}^{ls} \alpha [c_{f_t} - c_{f_l}] r_o \left( \frac{u_e}{u_{\infty}} \right)^2 dS + 2\pi \int_{ls}^{te} (c_{f_t}) r_o \left( \frac{u_e}{u_{\infty}} \right)^2 dS \right\} \quad (A8)$$

where

$S$  is the a vehicle arc-length dimension (feet),

$tr$  is the arc-length location of transition from laminar to turbulent flow (feet),

$ls$  is the arc-length location of laminar separation (feet),

and  $te$  is the total arc-length of the vehicle from the nose to the trailing edge (feet).

Total drag estimates for mixed viscous flow over an axisymmetric can be obtained from Equation (A8) once  $\alpha$  and the local laminar and turbulent skin friction coefficient distributions are known as a function of arc-length. For the LTA Vehicle, local skin friction coefficients were obtained from the TAPS Code. Two separate runs were performed with the code, the first for laminar flow to laminar separation and the second for the flow tripped at  $S = 21$  feet (based on the results presented in Section 4). The total drag of the vehicle hull was obtained from Equation A8, for  $\beta = 120$  degrees and for a turbulent growth angle of 10 degrees.